Fiber-matrix bond strength by pull-out tests on slag-based geopolymer with embedded glass and carbon fibers

Lais Alves, Nordine Leklou, Pascal Casari, Silvio de Barros

Fiber-matrix bond strength by pull-out tests on slag-based geopolymer with embedded glass and carbon fibers

Lais Alves[1a*], Nordine Leklou[2b], Pascal Casari[2c] and Silvio de Barros[1, 3d]

[1] *Federal Center of Technological Education (CEFET/RJ), Rio De Janeiro 20271-110, Brazil*

[2] *Institut de Recherche en Génie Civil et Mécanique, Université de Nantes, Saint-Nazaire 44600, France*

[3] *GeM Institute, UMR 6183 CNRS, CESI, Saint-Nazaire, France*

a)* corresponding author: lais.alves@cefet-rj.br, b) nordine.leklou@univ-nantes.fr, c) pascal.casari@univ-nantes.fr d) silvio.debarros@gmail.com

Keywords: blast furnace slag, cement Portland, sodium silicate activating solution, pull-out test, glass fiber, carbon fiber

Abstract. The reinforcement efficiency on a composite depends on the effective transfer of the stress between matrix and fiber. This work presents an experimental and comparative study of fiber-matrix bond strength for fiber-matrix interface between glass fibers and carbon fibers added to the slag-based geopolymer matrix. This analysis was performed by pull-out test. A total of 18 tests have been conducted, three for each type of fiber at each embedded length of 10 mm, 20 mm and 30 mm. The critical embedded length and the maximum interfacial shear (bond) strength were analyzed, and SEM observations were carried out for the cross-section of each fiber to measure diameter and observe the interface. It was found that the greatest efficiency was obtained by reinforcing with the glass fibers, incorporated at 20 mm in the slag-based matrix.

1. Introduction

The geopolymer began to be engendered in the 1970s by Davidovits, emerging as a new class of material derived from rocks and not from oil, as organic polymers [1]. It consists of inorganic polymers obtained by the alkaline activation of materials rich in silica (SiO_2) and alumina (Al_2O_3) [2] and have similar physical and mechanical characteristics as Cement Portland (CP) [3]. CP is the most used binder to produce cement and mortar, and the second most used material in the world, behind only water [4]. But the production process classifies it as the third-largest source of anthropogenic emissions of carbon dioxide (CO_2) [5]. In 2018, global process emissions reached 1.50 ± 0.12 Gt CO_2, which corresponds to about 4% of emissions from fossil fuels and cumulative emissions from 1928 to 2018 result in 38.3 ± 2.4 Gt CO_2, from which 71% occurred after 1990 [5]. Thus, the need to find an alternative material for construction processes arises.

Compared to CP, geopolymer emissions of CO_2 are approximately 43% less. Previous studies on these materials show that values for compressive strength are comparable [6 - 9], with values depending on the precursor material and activator solution. Correia et al. [10] found that geopolymers maintain considerable mechanical properties at temperatures up to 1000° C, whereas the application of most polymer resins is often limited to temperatures below 400° C. The material also presents high durability due to low apparent porosity, that results in low water permeability [11]. The main precursor materials are clays such as metakaolin [12 - 14] which is an artificially calcined kaolinite clay, and industrial waste such as blast furnace slag [14, 15] and fly ash [16 - 20].

Geopolymers have low tensile strength and low deformation capacity, which require the use of reinforcements [21]. Geopolymer matrix composites reinforced with particulates and fibers can be considered a solution to improve flexural strength and compressive strength [22 - 28]. The fibers increase the ductility of the material, preventing abrupt rupture [29]. Natural fibers, such as jute, and synthetic fibers, including glass and carbon fibers, can be used to reinforcement the geopolymer. There is a direct proportional relationship between the fiber-matrix interaction force, the strength, and the adhesion between the surface of the geopolymer matrix and the surface of the fiber [30 - 32].

The mechanical properties of fiber-reinforced composite materials highly depend by how efficient the load transfer through the interface between the fiber and the matrix [31, 33 - 36]. When a composite has a high adhesive force at the fiber-matrix interface, it exhibits high strength. This is due to a greater efficiency of the tension undergone by the matrix to the fibers. On the other hand, a high value of resulting stress (τ) causes the system to have a low tenacity, since the energy spent during the crack propagation is low, thus the failure of the matrix will propagate through the fiber-matrix interface. By analogy, it can be inferred that low values of τ result on low resistance, by the ineffective transfer of the tension to the fibers, and a high tenacity, since a high energy value would be expended not only by the cracks, but by the decoupling of the fiber [37].

A factor that influences the bond strength between the composite and the fiber is the critical embedded length (L_c) [4]. Fibers with shorter lengths results in deficiencies of the transmission of the external loads, besides causing debonding or decoupling. It can also be led to failures in regions that present lower values of resistance, either in the matrix or in the interface [38]. The critical length can be analyzed through the pull-out test and represents the optimum length capable of promoting the greater adhesion and better mechanical performance of the composite.

The analysis of the fiber-matrix adhesion can be performed through the study of the materials involved, their geometries, the loads, and the relative displacements, which provide the adhesion stress values [39], fundamental for the knowledge of the shear stress transfer between the fiber and the matrix. Different types of tests to study this interface have been developed, namely pull-out tests [40, 41], push-out tests [42, 43], micro-bond tests [44, 45] and fiber fragmentation tests [43, 46, 47]. The main difference between these tests is the test geometry [48]. However, the results analyzed by Pitkethly et. al [49] from different tests or from the same test applied by different researchers showed that the scatter was high.

To evaluate the bond quality at the fiber-matrix interface and the ability of stress transfer between the fiber and the matrix, the fiber pull-out test is one of the most important test methods developed [34]. The pull-out test is done by embedding the fiber up to a certain length into a specimen of the

matrix material. Then, the two ends are attached, the test body and the tip of the fiber, and a tensile force (F) is applied on the fiber. If the length of the fiber is greater than L_c, the fiber will break. Otherwise, the fiber slips from within the matrix without breaking. By pull-out test it is also possible to study the influence of fiber-matrix bond strength (τ), shear stress (μ) and shrinkage of the matrix by the pressure on the fiber (P_0) on the mechanical properties of the composite [34, 37].

Therefore, research work on fiber pull-out from a matrix is essential to understand the stress transfer on different types of composites. [34]. This work seeks to verify the interaction between a geopolymer slag-based matrix and synthetic glass and carbon fibers, comparing the fiber-matrix bond strength between the fiber and the matrix obtained by pull-out test. It aims to examine the cracking pattern of the fibers embedded in the specimens to discover the critical embedded length (L_c) and analyze relative displacements occurring at the fiber-matrix interface.

2. Materials and methods

This research used 100% ground blast furnace slag (GBFS), provided by ECOCEM from France, as the basic precursor material for the fabrication of the geopolymer paste specimens. The chemical composition for GBFS can be found in Table 1. Blast furnace slag is produced by drying and grinding granulated blast furnace slag. The degree of depolymerisation (DP) for the GBFS was found 1.44, which is an indicator of slag activity, that is considered good within a range from 1.3 to 1.5 [50]. D_{50} represents the average particle size in the production and application of powder materials, which can affect the durability of the geopolymer, since a large surface area leads to a higher polymerization rate and a difference in the number of voids [51]. For the GBFS used, D_{50} = 11.8 μm.

Table 1 - Chemical composition (%) of precursors

Precursor	**CaO**	**SiO_2**	**Al_2O_3**	**Fe_2O_3**	**MgO**	**Na_2O**	**SO_3**	**TiO_2**	**MnO**
GBFS	43.2	37.2	10.5	0.6	7	0.6	0.1	0.5	0.3

The alkaline activator solution employed in the mixtures, in its proper proportions, were prepared by mixing the sodium hydroxide (NaOH) solution with the sodium silicate (Na_2SiO_3) solution.

Sodium silicate (Na-Si) activator was prepared by mixing 10M sodium hydroxide (NaOH) with sodium silicate (Na_2SiO_3), maintaining a Na_2SiO_3/NaOH mass ratio of 2.0. The produced Na-silicate activator contained 66.7% water with 0.7 Na_2O/SiO_2 molar ratio. NaOH was purchased from ALFA-AESAR in the form of pellets, white colored with 98% purity. Sodium silicate (Na_2SiO_3) was purchased from VWR in soluble form, of pH between 11-11.5 and density 1.35 g/cm at 20ºC.

The precursor material (1,458.3 kg/m^3) was mixed for three minutes to have a more homogeneous mixture. Following, the activating solution (335.3 kg/m^3) mixed with the water (208.3 kg/m^3) was added to the dry mixture and blended for three minutes more. The percentage of water in the mixture was 12.4% and solid-to-liquid ratio 2.0.

The glass fiber used was commercial S2-glass which have high tensile strength of 3700 to 4300 MPa [52], without alkaline oxides, containing 65% SiO_2, 10% MgO and 25% Al_2O_3. The diameter for a single fiber was measured, by Scanning Electronic Microscopy (SEM), using ZEISS ЄVO®4 electron microscope equipped with a secondary electron sensor and a backscattered electrons sensor. After the pull-out test, prisms samples cores were sliced and polished into square shapes of 2cm×2cm by 0.5 cm thickness. Single glass fibers used measured around 17-20 µm and single carbon fibers had a diameter of 5-8 µm, as show in Figure 1. The fibers were not preconditioned as the aim was to study the interaction of the raw materials.

Figure 1 - Diameter of glass fiber (a) and carbon fiber (b) measured by SEM observations

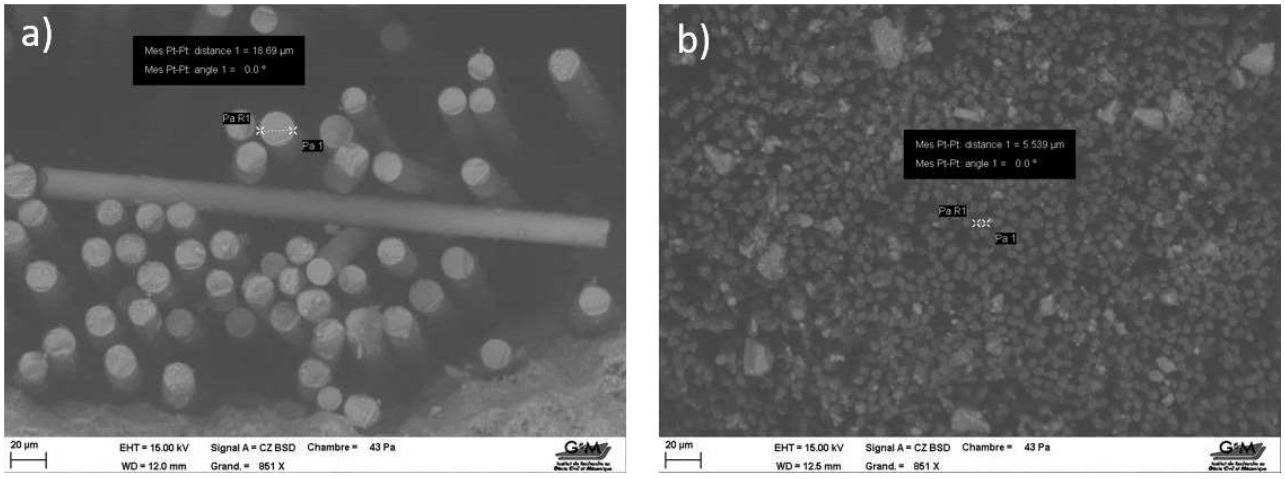

A total of 18 rectangular specimens were tested to find the critical embedded length and the maximum interfacial shear (bond) strength. Three essays were carried out for each type of fiber, carbon (CF) and glass (GF) at each embedded length of 10 mm, 20 mm and 30 mm [53]. The specimens were named according to the type of fiber used and the embedded length, e.g., for carbon fiber embedded 10 mm, specimen was named CF_10mm. The geopolymer paste specimens all had five cm in height and cross section of approximately one cm^2 [54]. Each fiber strand, composed of multiple fibers, had approximately one millimeter in diameter, measured by SEM observations [55]. The specimens were prepared at 20 ℃ and 50% humidity, demolded after 24 hours and kept in a plastic film until testing date. All the specimens were tested at seven days [54]. As observed in Alves [6], for this mixture, the GBFS had already been activated at this curing time.

A displacement of 0.5 mm/min [56, 57] was applied to the fiber on a Swift/Roell Z050 machine (Figure 2a), adapted with a Restrained Top Constraint (RTC) grapple, with a load cell of 50kN, following the schematics presented on Figure 2b (adapted from Yue [37]). While the force was applied, the behavior at the fiber-matrix interface was verified through the graph generated. The test was finished once the fiber is totally pulled-out of the matrix. The data obtained from the fiber pull-out test determines the applied loads from the shear stress and the relative displacements occurring at the fiber-matrix interface. With these results, it is possible to compute the relative adhesion stress and the strength effectiveness conferred by the fibrous reinforcement [58].

Figure 2 – Experimental setup of pull-out test (a) and pull-out test schematics (b)

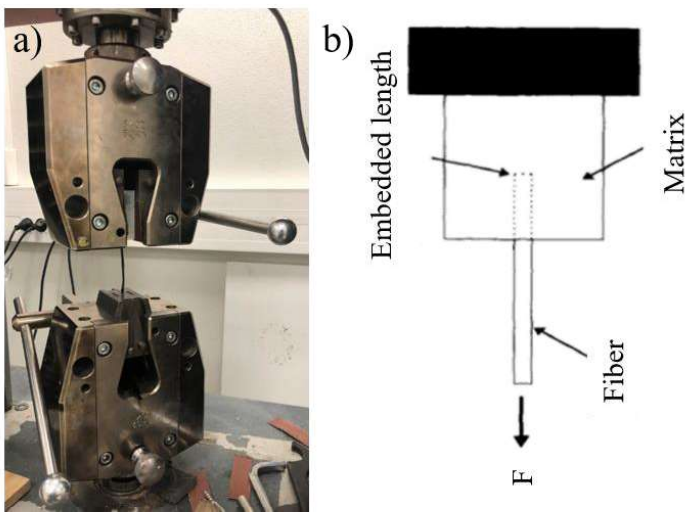

3. Results and discussion

Through the data analysis of the applied loads (F) and relative displacements (δ) that occur between the fiber and the matrix, it is possible to define the values of adhesion stress (τ) [39]. Compiled results, according to the embedded length of the reinforcing fiber, are shown in Table 2 (standard deviation values are in parentheses) and Figure 3.

Table 2 – Results for the different specimens of the pull-out test

Specimen	F (N)	δ (mm)	τ (MPa)
CF_10mm	22.77 (2.54)	3.04 (1.03)	0.7248 (0.1132)
CF_20mm	41.87 (4.03)	2.72 (0.28)	0.6664 (0.1745)
CF_30mm	45.32 (3.32)	1.39 (0.06)	0.4809 (0.1483)
GF_10mm	22.75 (3.87)	3.47 (0.17)	0.7242 (0.0863)
GF_20mm	76.42 (2.96)	2.82 (0.51)	1.2163 (0.1699)
GF_30mm	26.49 (5.12)	1.85 (0.70)	0.2811 (0.1311)

Figure 3 - Compiled values from the pull-out test

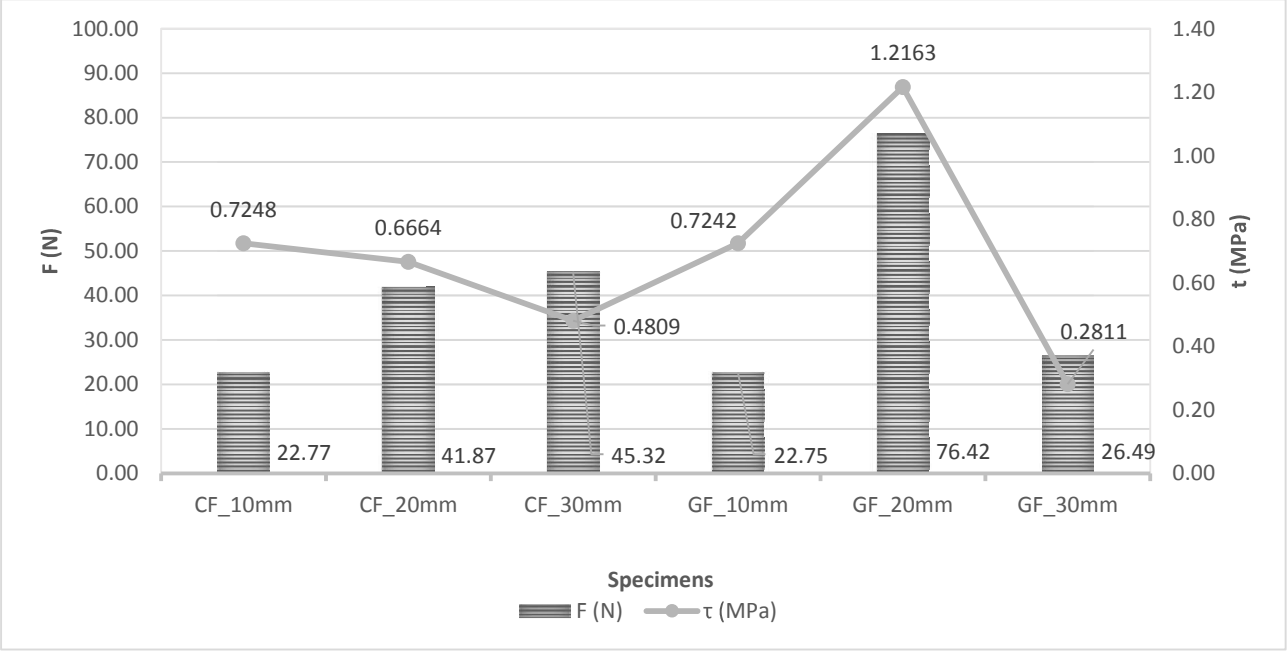

For specimens CF_10mm and CF_20mm the fiber was pulled out. Results show that the adhesion stress was higher for specimens with 10 and 20 mm of embedded length of carbon fiber, with values equal to 0.7248 and 0.6664 MPa, respectively. On specimen CF_30mm, the fiber fractured after reaching 45.32 N. For 30 mm length the lowest value for the adhesion stress was obtained reaching 0.4809 MPa. The values obtained show higher values of adhesion stress for composite CF_10mm,

but higher force for CF_30mm. Specimen CF_20mm presented the best adherence due to the higher value of applied load, without fiber fracture. Figure 4 shows SEM observations of the cross section and interface for one of the carbon fiber specimens with embedded length of 20 mm.

Figure 4 - SEM observations for cross section of carbon fiber (a) and interface after pull-out (b)

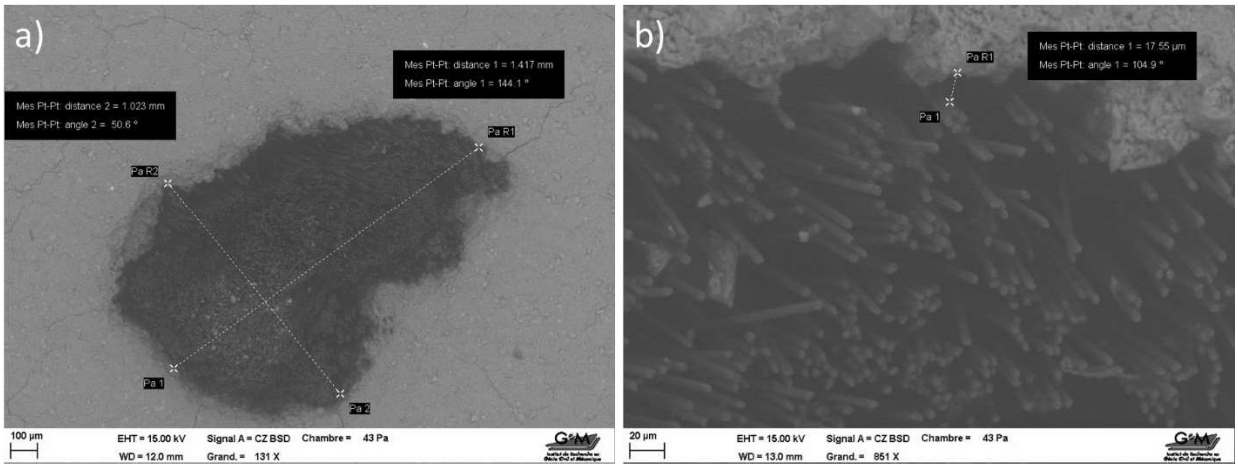

Glass fiber results showed same trend as that of carbon fiber. For specimens GF_10mm and GF_20mm the fiber was pulled out, with adhesion stress values of 0.7242 MPa and 1.2163 MPa, respectively. For 30 mm embedded length, a fracture on the fiber can be observed, at 26.49 N, due to the low value of 0.2811 MPa for adhesion stress. Thus, it is possible to affirm that the embedded length of 20 mm has the greatest capacity for transferring stresses between glass fiber and the matrix. Figure 5 shows SEM observations of the cross section and interface for one of the glass fiber specimens with embedded length of 20 mm.

Figure 5 - SEM observations for cross section of glass fiber (a) and interface after pull-out (b)

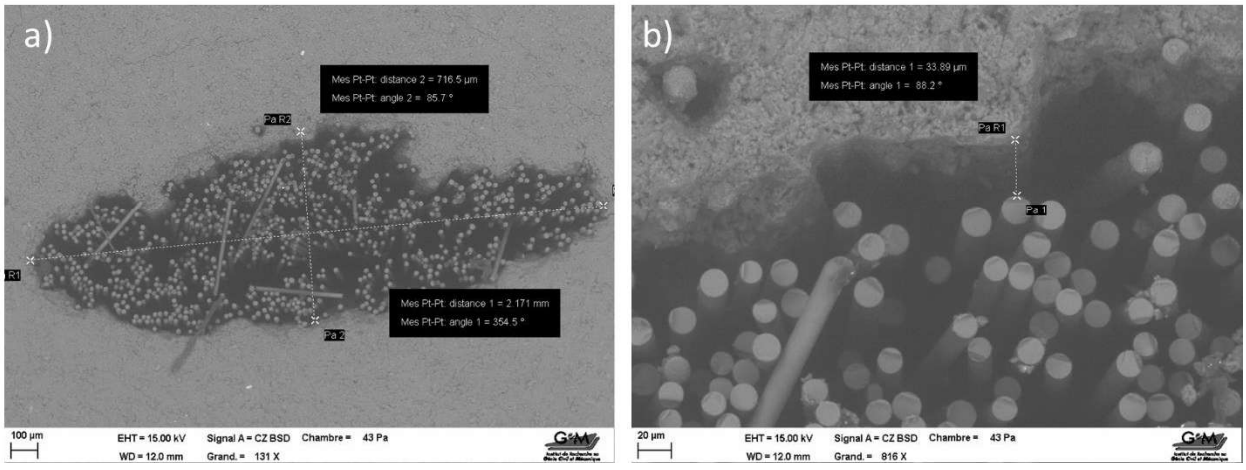

The critical length (L_c) is a possible explanation for the fact that the embedded lengths of 20 mm had higher stress transfer capacity between the fiber and the matrix [59]. Lengths below L_c present a deficiency in transfer of loads and the fiber slides through the matrix. For lengths above L_c, a greater interaction between the fibers can be noted, causing failure, entanglement and decrease of the effective length. According to Feih et. al [35], sizing controls the interface for glass fiber composites, because it is responsible for the physical-chemical link between the fiber surface and the matrix system.

The fiber material influences the efficiency of the reinforcement and of the displacement related to the applied load, due to chemical interactions [35] between the type of fiber and the matrix material. From the results, the fiber-matrix adhesion (τ) for the glass fiber system is better than for the carbon fiber system. This implies the glass fiber system has a matrix-to-fiber stress transfer more effective, which suggests higher tensile strength for the composite. Applied loads (F) and relative displacements (δ) are higher for glass fiber, which suggests higher toughness for the glass fiber composite, as observed from the larger values of τ. The applied load (F) vs displacement (δ) curve for the specimen CF_20mm, which presented bond strength and interaction in the fiber-matrix interface superior to the other specimens analyzed, is plotted in Figure 6.

Figure 6 – Pull-out test results for specimen GF_20mm

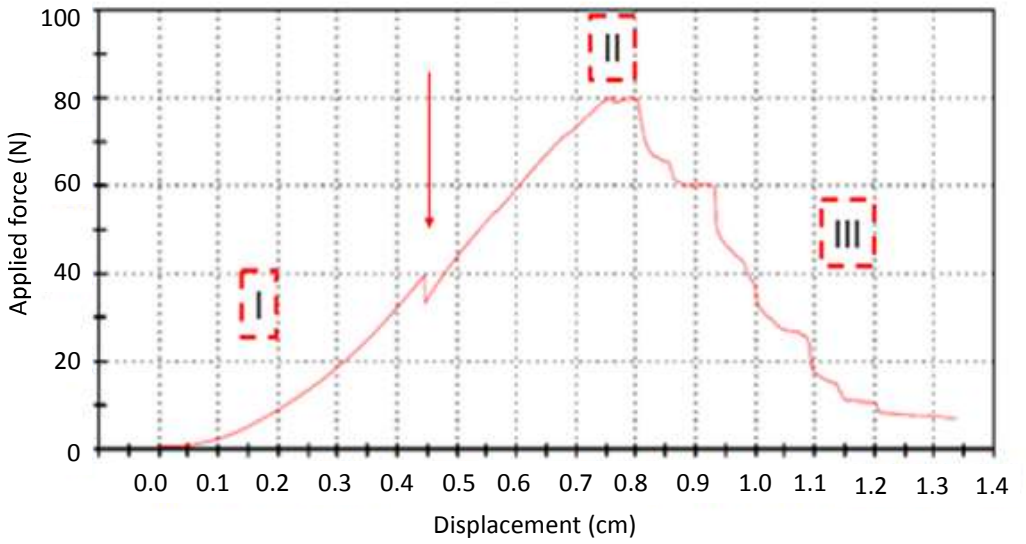

When studying the results for the specimen that presented the best adherence (Figure 6), it is important to notice that the pull-out test can be divided into three phases [37, 58]. The initial debonding and sliding phase, found in region I of the graph, is characterized by being an elastic-linear section, where the load is constantly increased until reaching a nonlinear stretch. Region II is qualified as maximum fiber stress, where the extraction force reaches the maximum value (F_{max}), and decohesion becomes partial. After this phase, there is a constant drop in the load, corresponding to region III. This region is controlled by the friction resistance of the interface and consists of sliding and pull-out until the fiber is extracted and completely withdrawn [37].

4. Conclusions

Understanding the interface properties helps in enhancing the structural properties of composite materials by improving the interfacial bonding. This work described a procedure to measure apparent interfacial shear strength from pull-out tests on fibrous reinforcements. The pull-out test provides results of fiber-matrix adhesion and interfacial properties that can characterize and assess fiber-reinforced composites. The interfacial parameters of applied loads (F), relative displacements (δ) and adhesion stress (τ) can be determined from pull-out data.

Two types of fiber were studied, glass fiber and carbon fiber, in three different embedded lengths of 10 mm, 20 mm and 30 mm. This study is fundamental to determine which material can be considered more efficient and makes the matrix more resistant to tensile and deformation strength. In addition to the different behaviors noticed due to the type fibers used, the influence of the embedded length of the fiber was another factor analyzed. The embedded length affects the load transfers and, therefore, the reinforcement efficiency. It is possible, through these data, to infer which composite has a more effective matrix-to-fiber stress transfer and determine the fiber critical embedded length.

It was concluded that the fiber that presented the best adherence for GBFS-based matrix is glass fibers, with 20 mm embedded length. The value obtained for adhesion stress of glass fiber at 20 mm embedded length is 68% higher than for glass fiber at 10 mm embedded length. When comparing with the carbon fiber system that has the higher value of applied load without fiber fracture, the glass

fiber system value corresponding to fiber-matrix interface is 83% higher. Critical length was considered 20 mm. With embedded lengths superior to the critical length, the fiber failure can occur before interface debonding. Lengths bellow critical length also causes deficiency in transfer of loads because there is a minimum critical length of the fiber required for a valid shear pull-out.

Acknowledgement

The authors acknowledge the Brazilian institutions CAPES (*Coordenação de Aperfeiçoamento de pessoal de nível superior* - Coordination of Improvement of senior staff), CNPq (*Conselho Nacional de Desenvolvimento Científico e Tecnológico* - National Council for Scientific and Technological Development) and *Institut de Recherche en Génie Civil et Mécanique* – Research Institute on Civil and Mechanical Engineering for the financial support and their support in conducting experiments.

References

1 Davidovits J (1993) From ancient concrete to geopolymers. In: Arts et Metiers Magazine, 180, p. 8-16

2 Alves LA, Nogueira A, Vazquez E, de Barros S (2020) A Bibliographic Historical Analysis on Geopolymer as a Substitute for Portland Cement. Key Engineering Materials, 834 : 127-131

3 Buchwald A, Zellmann H-D, Kaps C (2011) Condensation of Aluminosilicate Gels: model system for geopolymer binders. Journal of NonCrystalline Solids, v. 357, n. 5, p. 1376-1382

4 Nogueira A, de Barros S, Alves LA (2020) Fiber matrix adhesion on industrial geopolymer. Irianian Journal of Materials Science & Engineering 17(3): 95-101. DOI: 10.22068/ijmse.17.1.20

5 Andrew, RM (2019) Global CO2 emissions from cement production, 1928–2018. Earth Syst. Sci. Data. Preprint. DOI: 10.5194/essd-2019-152.

231 6 Alves L, Leklou N, de Barros S (2020) A comparative study on the effect of different
232 activating solutions and formulations on the early stage geopolymerization process. MATEC
233 Web of Conferences 322, 01039. DOI: 10.1051/matecconf/202032201039
234 7 Hardjito D, Rangan BV (2005) Development and properties of low-calcium fly ash-based
235 geopolymer concrete, Research Report, Perth, Australia: Curtin University of Technology
236 8 Duxson P, Fernandez-Jimenez A, Provis JL, Lukey GC, Palomo A, Van Deventer JSJ (2007)
237 Geopolymer Technology: The Current State of the Art, Material Science, 42, pp. 2917-2933
238 9 Pacheco-Torgal F, Castro-Gomes J, Jalali S (2008) Alkali Activated Binders: A review, Part
239 1, Historical Background, Terminology, Reaction Mechanisms and Hydration Products,
240 Construction and Building Materials, 22, pp. 1305-1314.
241 10 Correia EA, Torres SM, Alexandre MEO Gomes K.C., Barbosa N.P. and de Barros S. (2013)
242 Mechanical Performance of Natural Fibers Reinforced Geopolymer Composites. Materials
243 Science Forum 139-145.
244 11 Alves LA, Nogueira A, dos Santos J, de Barros S (2019) A Quick Overview on Geopolymer
245 Chemistry and General Properties. Res Dev Material Sci. 12(2). RDMS.000781.2019. DOI:
246 10.31031/RDMS.2019.12.000781
247 12 Hongling W, Haihong L, Fengyuan Y (2005) Synthesis and mechanical properties of
248 metakaolinite-based geopolymer. Colloids and Surfaces A: Physicochem. Eng. Aspects 268:
249 1–6
250 13 Pappalardo Jr. A, Jalali S, Silva FJ, Schmeling RM (2014) Interrelationship between
251 Architecture, Structures, Fabrication and Construction using sustainable materials.
252 Proceedings of the IASS-SLTE 2014 Symposium, Brasília, Brazil.
253 14 Mauri J, Dias DP, Cordeiro GC, Dias AA (2009) Geopolymer mortar: degradation study by
254 sodium sulfate and sulfuric acid (in Portuguese). Revista Matéria 14(3): 1039 – 1046.

15 Salih MA, Ali AAA, Farzadnia N (2014) Characterization of mechanical and microstructural properties of palm oil fuel ash geopolymer cement paste. Construction and Building Materials 65: 592–603

16 Krishnan L, Karthikeyan S, Nathiya S, Suganya K (2014) Geopolymer concrete an eco-friendly construction material. IJRET: International Journal of Research in Engineering and Technology 3(11):164-167

17 Rangan BV (2014) Geopolymer concrete for environmental protection. The Indian Concrete Journal 88(4): 41-59.

18 Sreevidya V, Anuradha R, Venkatasubramani R, Yuvaraj S (2014) Flexural behavior of geopolymer ferrocement elements. Asian Journal Of Civil Engineering (BHRC) 15(4): 563-574

19 Olivia M, Nikraz HR (2011) Strength and water penetrability of fly ash geopolymer concrete. ARPN Journal of Engineering and Applied Sciences 6 (7): 70-78

20 Shaikh FUA (2016) Mechanical and durability properties of fly ash geopolymer concrete containing recycled coarse aggregates. International Journal of Sustainable Built Evironment 5: 277-287

21 Sakulich AR (2011) Reinforced geopolymer composites for enhanced material greenness and durability. Sustainable Cities and Society 1: 195– 210

22 Natali A, Manzi S, Bignozzi. MC (2011) Novel fiber-reinforced composite materials based on sustainable geopolymer matrix. Procedia Engineering 21: 1124-1131

23 Metha PK, Monteiro PJML (2006) Concrete: Microstructure, Properties, and Materials. McGraw-Hill Publishing, Ed. 3, United States

24 He PG, Jia DC, Lin TS (2010) Effects of high-temperature heat treatment on the mechanical properties of unidirectional carbon fiber reinforced geopolymer composites, Ceram. Int. 36 (4) 1447–1453.

280 25 Silva FJ and Thaumaturgo C (2003) “Fibre reinforcement and fracture response in
281 geopolymeric mortars” Fatigue Fract. Engng. Mater. Struct. 26: 167-172.
282 https://doi.org/10.1046/j.1460-2695.2003.00625.x
283 26 Zhang YS, Sun W and Li ZJ (2006) Impact behavior and microstructural characteristics of
284 PVA fiber reinforced fly ash-geopolymer boards prepared by extrusion technique,
285 J.Mater.Sci.41 (10) 2787–2794.
286 27 Lin TS, Jia DC, He PG (2003) Thermo-mechanical and microstructural characterization of
287 geopolymers with α-Al2O3 particle filler, Int. J. Thermophys (30) 1568–1577.
288 28 Alomayri T, Shaikh FUA, Low IM (2014) Mechanical and thermal properties of ambient
289 cured cotton fabric-reinforced fly ash-based geopolymer composites, Ceram. Int.40 (9)
290 14019–14028.
291 29 Silva F (2009) Cracking mechanisms in durable sisal fiber reinforced cement composites. In:
292 Cement and Concrete Composites, v. 31, n. 10 p. 721-730
293 30 Bakis CE, Bank LC, Brown VL, Cosenza E; Davalos JF, Lesko JJ, Machida A, Rizkalla SH,
294 and Triantafillou TC (2002) Fiber-Reinforced Polymer Composites for Construction—State-
295 of-the-Art Review. In: J. Compos. Constr., 2002, 6(2): 73-87. DOI: 10.1061/(ASCE)1090-
296 0268(2002)6:2(73)
297 31 Kessler A, Bledzki AK (2000) Correlation between interphase-relevant tests and the impact-
298 damage resistance of glass/epoxy laminates with different surface treatments. Compos Sci
299 Technol 60 (1): 125–30.
300 32 DiBenedetto AT (2001) Tailoring of interfaces in glass fiber-reinforced polymer composites:
301 a review. Mater Sci Eng A—Struct Mater Prop Microstruct Process 302 (1): 74–82.
302 33 Zhandarov S, Pisanova E, Mäder E, Nairn JA (2000) Investigation of load transfer between
303 the fiber and the matrix in pull-out tests with fibers having different diameters. J. Adhesion
304 Sci. Technol., Vol. 15, No. 2, pp. 205–222

305 34 Fu S-Y, Lauke B (1999) Comparison of the stress transfer in single- and multi-fiber composite
306 pull-out tests. J. Adhesion Sci. Technol., Vol. 14, No. 3, pp. 437–452. DOI:
307 10.1163/156856100742690
308 35 Feih S, Wei J, Kingshott P, Sorensen BF (2005) The influence of fibre sizing on the strength
309 and fracture toughness of glass fibre composites. Composites Part A 36: 245-255
310 36 Jones FR (2002) Glass fibres. In: Hearle JWS, editor. High performance fibres. Cambridge:
311 Woodhead Publishing Limited; p. 191–238]
312 37 Yue CY, Looi HC, Quek MY (1995) Assessment of fibre-matrix adhesion and interfacial
313 properties using the pull-out test. Int. J. Adhesion and Adhesives 15: 73-80
314 38 Stamboulis A, Baillie C, Schulz E (1999) Interfacial characterisation of flax fibre-
315 thermoplastic polymer composites by the pull-out test. Die Angewandte Makromolekulare
316 Chemie, 272(4759):117–120
317 39 Silva F (2011) Effect of fiber shape and morphology on interfacial bond and cracking
318 behaviors of sisal fiber cement-based composites. In: Cement and Concrete Composites, v.
319 33, n. 8: 814-823
320 40 Quentin V, Esposito A, Saiter JM, Santulli C, Turner J (2018) Interfacial Characterization by
321 Pull-Out Test of Bamboo Fibers Embedded in Poly (Lactic Acid). Fibers 6
322 doi:10.3390/fib6010007
323 41 Zhandarov S, Pisanova E, Mäder E, Nairn JA (2001) Investigation of load transfer between
324 the fiber and the matrix in pull-out tests with fibers having different diameters. Journal of
325 adhesion science and technology, 15(2):205–222
326 42 Parthasarathy TA, Jero PD, Kerans RJ (1991) Extraction of Interface Properties from a Fiber
327 Push-Out Test. Scripta Metall Mater. vol. 24: 2315–2318
328 43 Zhou XF, Wagner HD, Nutt SR (2001) Interfacial properties of polymer composites measured
329 by push-out and fragmentation tests. Composites Part A: Applied Science and Manufacturing,
330 32(11):1543–1551

331 44 Sockalingam S, Nilakantan G (2012) Fiber-Matrix Interface Characterization through the
332 Microbond Test: A Review. International Journal of Aeronautical and Space Sciences,
333 13(3):282–295
334 45 Zhandarov SF, Mäder E, Yurkevich OR (2002) Indirect estimation of fiber/polymer bond
335 strength and interfacial friction from maximum load values recorded in the microbond and
336 pull-out tests. Part I: local bond strength. J. Adhesion Sci. Technol., Vol. 16, No. 9, pp. 1171–
337 1200
338 46 Huber T, Müssig J (2008) Fibre matrix adhesion of natural fibres cotton, flax and hemp in
339 polymeric matrices analyzed with the single fibre fragmentation test. Composite Interfaces,
340 15(2-3):335–349
341 47 Kim BW, Nairn JA (2002) Observations of Fiber Fracture and Interfacial Debonding
342 Phenomena Using the Fragmentation Test in Single Fiber Composites. J. of Comp. Mat. 36
343 (15): 1825-1858 doi: 10.1177/0021998302036015243
344 48 Zhandarov SF, Mäder E (2005) Peak force as function of the embedded length in pull-out and
345 microbond tests: effect of specimen geometry. J. Adhesion Sci. Technol., Vol. 19, No. 10, pp.
346 817–855
347 49 M. J. Pitkethly, J. P. Favre, U. Gaur, J. Jakubowski, S. F. Mudrich, D. L. Caldwell, L. T.
348 Drzal, M. Nardin, H. D.Wagner, L. DiLandro, A. Hampe, J. P. Armistead, M. Desaeger and
349 I. Verpoest, (1993) A Round-Robin Programme on Interfacial Test Methods. Composites Sci.
350 Technol. 48, 205–214.
351 50 Duxson P, Provis JL (2008) Designing Precursors for Geopolymer Cements. J. Am. Ceram.
352 Soc. 91: 3864–3869.
353 51 Lateef N. Assi, Deaver E., Mohamed K. ElBatanouny, Ziehl P (2016) Investigation of Early
354 Compressive Strength of Fly Ash-Based Geopolymer Concrete. Construction and Building
355 Materials 112: 807-815. http://dx.doi.org/10.1016/j.conbuildmat.2016.03.008

52 Advanced Glassfiber Yarns, Product Information (2000) “High Temperature 933 S-2 Glass Roving”

53 Zulfiati R, Saloma, Idrid Y (2019) Mechanical properties of fly-ash based geopolymer with natural fiber. IOP Conf. Series: J. of Physics: Conf. Series 1198: 082021 doi: 10.1088/1742-6596/1198/8/082021

54 Trindade ACC (2017) Development and mechanical behavior of textile geopolymer composites reinforced with jute fiber [in Portuguese]. PUC-Rio, Rio de Janeiro, Brazil.

55 Nguyen DC, Makke A, Montay G (2015) A Pull-out Fiber/Matrix Interface Characterization of Vegetal Fibers Reinforced Thermoplastic Polymer Composites: The Influence of the Processing Temperature. Int. J. of Chem., Mol., Nuc., Mat. And Metall. Eng. 9 (6): 732:736

56 Liu Y, Ma Y, Yu J, Zhuang J, Wu S, Tong J (2019) Development and characterization of alkali treated abaca fiber reinforced friction composites. Composite Interfaces, 26:1, 67-82, DOI: 10.1080/09276440.2018.1472456

57 Lima RAA. Structural monitoring of helicopter rotor blades using intelligent materials [in Portuguese]. CEFET/RJ, Rio de Janeiro, Brazil.

58 Sorensen BF, Lilholt H (2016) Fiber pull-out test and single fiber fragmentation test – analysis and modelling. IOP Conf. Series: Mat. Sci. and Eng. 139: 012009 doi:10.1088/1757-899X/139/1/012009

59 Sharan Chandran M., Padmanabhan K., Dipin Raj D. K., Yashasvi Chebiyyam (2019): A comparative investigation of interfacial adhesion behaviour of polyamide based self-reinforced polymer composites by single fibre and multiple fibre pull-out tests, Journal of Adhesion Science and Technology, DOI: 10.1080/01694243.2019.1672467